Charge-Transfer Mechanism for Cytochrome *c* Adsorbed on Nanometer Thick Films. Distinguishing Frictional Control from Conformational Gating

By: Dimitri E. Khoshtariya, Jianjun Wei, Haiying Liu, Hongjun Yue and David H. Waldeck

D. E. Khoshtariya, J. Wei, H. Y. Liu, H. J. Yue, and D. H. Waldeck, "The Charge-Transfer Mechanism for Cytochrome C Adsorbed on Nanometer Thick Films. Distinguishing Frictional Control from Conformational Gating" *J. of American Chemical Society*, 2003, 125, 7704-7714.

Abstract:

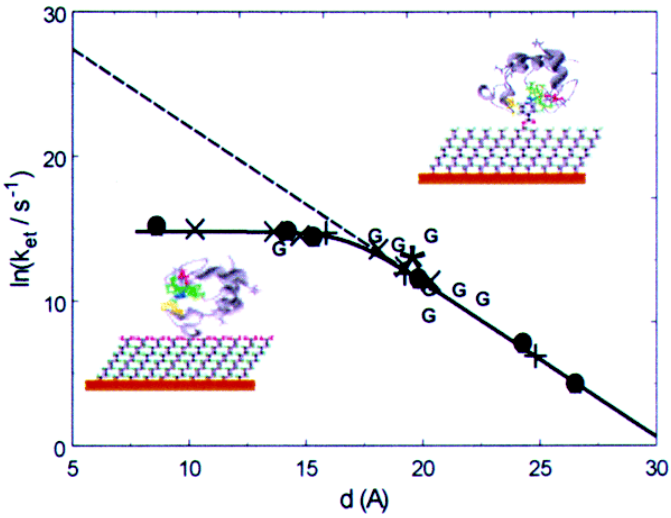

Using nanometer thick tunneling barriers with specifically attached cytochrome *c*, the electrontransfer rate constant was studied as a function of the SAM composition (alkane versus terthiophene), the ω-terminating group type (pyridine, imidazole, nitrile), and the solution viscosity. At large electrode-reactant separations, the pyridine terminated alkanethiols exhibit an exponential decline of the rate constant with increasing electron-transfer distance. At short separations, a plateau behavior, analogous to systems involving -COOH terminal groups to which cytochrome *c* can be attached electrostatically, is observed. The dependence of the rate constant in the plateau region on system properties is investigated. The rate constant is insensitive to the mode of attachment to the surface but displays a significant viscosity dependence, change with spacer composition (alkane versus terthiophene), and nature of the solvent (H_2O versus D_2O). Based on these findings and others, the conclusion is drawn that the charge-transfer rate constant at short distance is determined by polarization relaxation processes

in the structure, rather than the electron tunneling probability or large-amplitude conformational rearrangement (gating). The transition in reaction mechanism with distance reflects a gradual transition between the tunneling and frictional mechanisms. This conclusion is consistent with data from a number of other sources as well.

Keywords: cytochrome *c* | electron transfer rate constant | charge-transfer rate constant | nanometer thick tunneling barriers

Article:

1. Introduction

Because of their diversity and rich behavior, the kinetics and mechanism of biochemical charge-transfer processes are often difficult to identify, and many aspects of a protein's microscopic mechanism remain unclear because of the complex and inhomogeneous character of biomolecular systems. Nevertheless, experimental and theoretical studies have shown that elementary electron-transfer events involving redox-active proteins can be understood in the light of contemporary theoretical models for molecular charge-transfer reactions. Cytochrome *c* is a small, “model”, redox protein[1] with a well-known molecular structure, and numerous studies of its electron-transfer rate have been performed, both homogeneous[2,3] and heterogeneous.[4,5]

A large number of studies have compared cytochrome *c*'s electron-transfer kinetics with contemporary theoretical models. The nonadiabatic (tunneling) charge-transfer mechanism[6] predicts the exponential decay of the charge-transfer rate constant with the electron-transfer distance R_e

$$k_{et} \propto \exp[-\beta(R_e - R_o)] \qquad (1)$$

where R_o is a minimal electron donor−acceptor distance and β is a decay parameter whose value depends on the intervening atomic and molecular structure.[7] The observation of an exponential distance dependence for a given reaction series provides strong evidence for the nonadiabatic (tunneling) mechanism. The exponential dependence arises from the dependence of the rate constant on the electronic coupling $|V|$ between the electron donor and acceptor

$$k_{et} \propto |V|^2 \qquad (2)$$

and the exponential decrease of the exchange interaction that causes $|V|$, such that

$$|V| = V^0 \exp\left[-\frac{\beta}{2}(R_e - R_o)\right] \qquad (3)$$

where V^0 is the value of |V| at the minimum distance R_o. The same model predicts an activation free energy for the rate constant

$$k_{et} \propto \exp\left[-\frac{\Delta G_a}{RT}\right] \qquad (4)$$

that depends quadratically on the reaction free energy ΔG_o, namely

$$\Delta G_a = \frac{(\lambda - \Delta G_o)^2}{4\lambda} - |V| \qquad (5)$$

Assuming that the reorganization free energy, λ, is constant within a reaction series, a bell-shaped dependence of $\log(k_{et})$ vs ΔG_o should be observed, at least for "homogeneous" unimolecular rate constants (for electrode processes eq 5 is approximately valid within the range of $|\Delta G_o| \leq \lambda$, *vide infra*[8]).

An alternative description of the electron-transfer rate constant is required when the electronic interaction between the electron donor and electron acceptor is large enough and is referred to as the adiabatic limit. In this limit, the rate constant is no longer controlled by the magnitude of the electronic coupling but rather by the frictional coupling between the changing charge distribution of the reactants and the polarization of the surrounding medium. This frictional coupling is most often characterized by a characteristic relaxation time of the medium τ_s or a viscosity η for the medium. Phenomenological and theoretical models, based on the Kramers treatment,[9] have been used to treat the reaction rate constant in this limit. When the frictional coupling to the medium is very strong, the rate constant decreases as $1/\tau_s$ or $1/\eta$. Empirically, a power law form is often found to describe the friction dependence of the rate constant; for example,

$$k_{et} \propto \eta^{-\gamma} \qquad (6)$$

where γ is an "empirical" parameter with typical values within the range $0 < \gamma \leq 1$.[10]

The electron-transfer kinetics of cytochrome *c* in "homogeneous" systems, including bimolecular reactions of the protein with natural or artificial counterparts[3] and unimolecular reactions of an unnatural cytochrome that has low-molecular weight redox partners covalently attached,[2] have been performed. Although these studies have provided a wealth of information and indicate biases toward one or more of the characteristic features quantified by eqs 1, 5, or 6, they do not probe the dependence of the intrinsic charge-transfer mechanism on the reaction conditions. Except for a few reports (*vide infra*), these studies do not explore the possible change in the mechanism from the nonadiabatic limit to the adiabatic limit. This deficiency reflects the difficulty in varying the fundamental parameters, R_e, $|V|$, and ΔG_0 in an independent and quantifiable manner. Heterogeneous bioelectrochemical systems in which cytochrome *c* or other redox proteins exchange electrons with a metal electrode by tunneling through insulating self-assembled monolayer (SAM) films promises to allow such studies.[4,5,11] Electrochemical methods are well proven for the determination of rate constants and intrinsic mechanisms in chemical studies.[10,12]

The present work is an extension of earlier studies from this group that probes the electron-transfer kinetics of cytochrome *c* that is linked to nanometer thick monolayer films by direct

binding with the protein's heme unit.[5,11] This report presents new data on the viscosity dependence and deuterium isotope dependence of the electron-transfer rate constant for the systems described earlier and presents data for new types of tethers, including a conjugated linker (Chart 1). In addition to these new data, a comprehensive and self-consistent analysis of the results is presented. In particular, the data show a clear change in the reaction mechanism with the distance of the protein from the electrode, and the analysis compares the description by a unified charge-transfer theory with that by a conformational gating model.

Chart 1. Molecular Structures Are Shown for the Different Receptor-Based Tethering Molecules

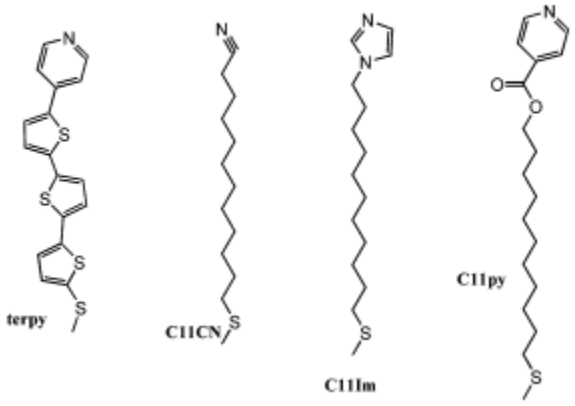

2. Experimental Section

Reagents and Materials. Water for the experiments was purified by using a Barnstead−Nanopure system and had a resistivity of 18 MΩ cm. 1,3-Dicyclohexylcarbodiimide, DCC, (99%) was purchased from Alfa Aesar. All mercaptoalkanes were purchased from Aldrich and used without further purification. Imidazole (99%), 6-mercapto-1-hexanol, 11-bromo-1-undecanol (98%), 1-nonadecanol, isonicotinic acid (99%), docosanedioic acid (85%), methanolic iodine (99%), sodium bisulfite (99%), thiourea (99+%, A.C.S. reagent), K_2CO_3 (99+%, A.C.S. reagent), NaOH (97%), and $MgSO_4$ (99%) were purchased from Aldrich. 4-Pyridinecarbaldehyde and 2-bromothiophene, 4- bromopyridine anhydrous *N*,*N*-dimethylformamide (DMF) were bought from Fluka. Absolute ethanol was purchased from Pharmcoproducts, Inc.; Dextrose ((+)-D-glucose anhydrous, 99%) was purchased from Sigma.

Cytc (Sigma C 7752, from horse heart, minimum 95% based on molecular weight 12 384) was purified using a cation exchange column (CM-52, carboxymethyl−cellulose from Whatman) in a manner described previously.[11] The purified cytochrome *c* was stored under an argon atmosphere in a freezer with dry ice until use.

The solution used in the voltammetry study was 20 mM sodium phosphate buffer solution at pH 7. The viscosity of the solutions was varied by using glucose concentrations of 0 g/L, 200 g/L, and 400 g/L. The solution viscosities were measured to be 0.98 cP, 1.76 cP, and 3.88 cP, respectively. The measurements were performed at room temperature with an Ubbelohde viscometer.

Electrode Preparation. More details of preparation and characterization of the gold electrode can be found elsewhere.[11] Only a brief outline of the procedure is given here. A gold wire (0.5 mm diameter, 99.99%) was cleaned by reflux in nitric acid (68−70%) at 130 °C overnight and then was washed with deionized water. The tip of the gold wire was heated and annealed in a gas flame to form a ball of about 0.06−0.12 cm^2 surface area. Chemically modified electrodes were prepared by immersion in an ethanol or THF solution that contained 1 mM $-S(CH2)_nOOC(C_5H_4N)$ and $-S(CH2)_{n-2}CH_3$ (the mole ratio of $-S(CH2)_nOOC(C_5H_4N)$ to $-S(CH2)_{n-2}CH_3$ was 1:9). The electrode remained in this solution for 1 day to form the mixed SAM. The electrode was taken out from the solution, first rinsed with absolute ethanol (or THF), then rinsed with the supporting buffer solution (20 mM phosphate buffer pH 7), and finally dried by a stream of argon gas. The electrode was characterized, as previously,[11] and then immersed in a 100 μM cytochrome *c* solution (purged with argon gas) for 30−60 min in order to immobilize the cytochrome on the SAM-coated electrode. These electrodes were immediately used in voltammetry studies.

Electrochemical Measurements. Electrochemical measurements were performed by using an EG&G PAR-283 potentiostat controlled by a PC computer running version 4.3 of PARC's 270 software and a GPIB board. The three-electrode cell was composed of a platinum spiral counter electrode, an Ag/AgCl (3 M NaCl) reference electrode, and the SAM-coated Au as a working electrode. The voltammetry measurements were performed in 20 mM phosphate buffer solution (pH of 7.0) at different viscosities under an argon atmosphere. To study the isotope effects, the SAM modified gold electrodes were incubated in cytochrome *c* D_2O buffer solution to immobilize protein and then measured in both D_2O and H_2O buffer solution.

Material Preparation. Pyridine, imidazole, nitrile terminated disulfide derivatives, 2-(4-pyridine-5-terthiophene-thiol), nonadecanethiol, and heneicosanethiol were prepared according to literature procedures.[11,13] 12-Mercapto-1-dodecanol was prepared in the manner reported earlier.[11a] ^1H NMR spectra were obtained at 300 MHz, and the coupling constant is reported in Hz.

1. Preparation of Disulfides. A. Bis(6-hydroxyhexanyl)disulfide: 6-Mercapto-1-hexanol (6.0 g, 44.696 mmol) was dissolved in 10 mL of methanol and titrated with 0.5 M methanolic iodine until the reaction turned from colorless to a persistent yellow. The reaction was quenched with 10% sodium bisulfite to a colorless solution. The resulting mixture was dissolved in distilled water and extracted with CH_2Cl_2, and the solvent was removed under vacuum. Purification of the resulting crude disulfide was performed by flash chromatography (CH_3Cl) to afford the disulfide (5.35 g) as a white solid in 90% yield. ^1H NMR (300 MHz) $CDCl_3$ δ 3.649 (t, J = 6.435, 4H); 2.690 (t, J = 7.275, 4H); 1.703 (m, 4H); 1.584 (m, 4H); 1.510−1.375 (m, 8H).

B. Bis(11-hydroxyundecyl)disulfide: ^1H NMR (300 MHz) $CDCl_3$ δ 3.651 (q, J = 6.18, 4H); 2.689 (t, J = 7.34, 4H); 1.679 (m, 4H); 1.579 (m, 4H); 1.379−1.290 (broad, 28 H).

C. Bis(16-hydroxyhexadecyl)disulfide: 16-Mercaptohexadecanol was prepared by reducing 16-mercaptohexadecanoic acid in ethyl ether using $LiAlH_4$. Diluted NaOH solution was used to quench the reaction. The resulting solution was dissolved in 0.2 M HCl and extracted with CH_2Cl_2. The solvent was removed under vacuum. Purification of the resulting crude 16-

mercaptohexadecanol was performed by flash chromatography (CH_3Cl). ^1H NMR (300 MHz) $CDCl_3$ δ 3.646 (t,*J* = 6.615, 2H); 2.527 (q, *J* = 7.34, 2H); 1.603 (m, 6H); 1.327 (broad, 23H). Bis(16-hydroxyhexadecyl)disulfide is insoluble in common solvents, such as CH_2Cl_2, and NMR data were not obtained.

D. Bis(20-hydroxyeicosyl)disulfide and Bis(22-hydroxydocosyl)disulfide were prepared through the same procedures as that for the preparation of Bis(16-hydroxyhexadecyl disulfide.

2. **Preparation of Pyridine Derivatives. A. Bis[6-((pyridinylcarbonyl)oxy)hexanyl]disulfide:**1,2-dicyclohexylcarbodiimide (DCC) (4.13 g, 20.02 mmol) was added to 20 mL of dichloromethane solution of bis(6-hydroxyhexanyl)disulfide (2.42 g, 9.10 mmol), isonicotic acid (2.24 g, 18.20 mmol), and 4-(dimethylamino)pyridine (0.22 g, 1.82 mmol) at 0 °C. After 1 h, the solution was allowed to warm to room temperature, and stirring was continued for 4 days. After removal of the precipitated dicyclohexylurea (DCU) by filtration, the solvent was removed under reduced pressure to yield a crude solid. The solid was recrystallized with ethanol and chromatographed on silica gel (60−200 mesh) with ethyl acetate. Evaporation of the solvent yielded the disulfide as 3.45 g of a white solid. ^1H NMR (300 MHz) $CDCl_3$ δ 8.789 (d, *J* = 5.97, 4H); 7.849 (d, *J* = 5.97, 4H); 4.362 (t, *J* = 6.615, 4H); 2.695 (t, *J* = 7.215, 4H); 1.802 (m, 4H); 1.723 (m, 4H); 1.488−1.453 (m, 8H).

B. Bis[11-((4-methyl-4-pyridinylcarbony)oxy)undecyl]disulfide, Diiodides: Bis[11-((4-pyridinylcarbonyl)oxy)undecyl]disulfide was refluxed with an excess of iodomethane in ethanol for 24 h under nitrogen. The solution was cooled to room temperature, and the precipitate that formed was filtered and recrystallized in ethanol and acetone 3 times. A brown solid was obtained. ^1H NMR (300 MHz) $CDCl_3$ δ 9.501 (d, *J* = 6.54, 4H); 8.515 (d, *J* = 6.46, 4H); 4.834 (s, 6H); 4.449 (t, *J*= 6.614, 4H); 2.694 (t, *J* = 7.301, 4H); 1.818 (m, 4H); 1.678 (m, 8H); 1.476−1.216 (broad, 24H).

C. Bis[11-((4-pyridinylcarbonyl)oxy)undecyl]disulfide: ^1H NMR (300 MHz) $CDCl_3$ δ 8.810 (s, 4H); 7.901(d, *J* = 5.73, 4H); 4.367 (t, *J* = 6.63, 4H); 2.684 (t, *J* = 7.32, 4H); 1.789 (m, 4H); 1.675 (m, 4H); 1.43−1.29 (broad, 28H). EI−HRMS: calcd 616.3385 ($C_{34}H_{52}N_2O_4S_2$), found 616.3369.

D. Bis[16-((4-pyridinylcarbony)oxy)hexadecyl]disulfide: ^1H NMR (300 MHz) $CDCl_3$ δ 8.889 (s, 4H); 7.869 (d, *J* = 5.46, 4H); 4.359 (t, *J* = 6.705, 4H); 2.683 (t, *J* = 7.36, 4H); 1.781 (m, 8H); 1.673 (m, 4H); 1.43−1.29 (broad, 44H). EI−HRMS: calcd 756.4896 ($C_{44}H_{72}N_2O_4S_2$), found 756.4934.

E. Bis[22-((4-pyridinylcarbony)oxy)docosyl)disulfide: ^1H NMR (300 MHz) $CDCl_3$ δ 8.789 (d, *J*= 5.52, 4H); 7.857 (d, *J* = 5.76, 4H); 4.358 (t, *J* = 6.66, 4H); 2.685 (t, *J* = 7.37, 4H); 1.784 (m, 4H); 1.694 (m, 4H); 1.26 (broad, 72H).

F. 2-(4-Pyridine-5-terthiophene-thiol): Details on the preparation of the terthiophene will be reported elsewhere.

3. Results

Two different strategies have been used to adsorb cytochrome *c* onto the surface of nanometer thick insulating films on metal electrodes (see Figure 1). The first method uses carboxylate terminated SAMs that bind the protein electrostatically, since it is positively charged (left panel). It is believed that the ionized lysines on the surface of the cytochrome interact with the carboxylate groups. The second method uses SAMs that are terminated with nitrogen containing headgroups that can bind to the heme unit of the protein (right panel). The first method has the advantage of providing a better mimic of the in vivo environment of cytochrome *c*, and the distribution of lysines on the surface leads to an adsorption geometry that has the heme edge oriented toward the surface.[14] The second method provides control of the cytochrome *c* orientation on the surface and directly "wires" the heme to the electrode but requires the receptor group on the SAM to displace an axial ligand from the heme, thereby causing partial unfolding. The second method is exploited here, but comparisons are drawn with the work of others using the first method.

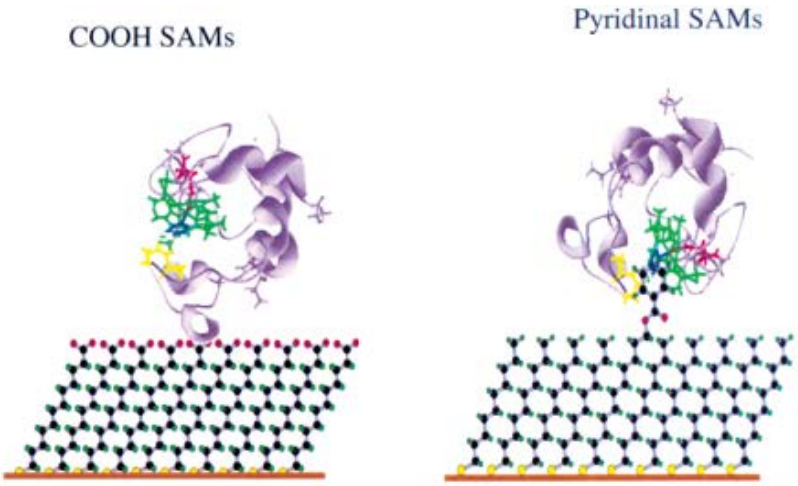

Figure 1. This schematic drawing shows the adsorption of the cytochrome *c* to the surface of self-assembled monolayer films through two different binding motifs: (left panel) electrostatic attraction between carboxylate groups on the SAM and the protein's positive lysine groups and (right panel) coordination of a receptor group (pyridine) in the SAM with the heme of the protein.

The standard rate constants for electron transfer between the SAM coated Au electrode and the attached cytochrome *c* were determined through the evaluation of cyclic voltammetry data, a standard procedure.[12] Representative voltammograms for these systems have been reported.[5,11] In brief, the dependence of the observed peak potential for the faradaic current is measured as a function of the voltage scan rate.[15] Quantitative analysis of this dependence provides the standard heterogeneous electron-transfer rate constant, which is the heterogeneous electron-transfer rate constant at a reaction free energy of zero. Plots of the peak position as a function of scan rate have been reported for the alkylpyridine systems, already.[5] This method is limited in its time resolution by the RC characteristics of the electrode. With the small diameter (*ca*. 1 mm) gold ball electrodes used in this work, rate constants up to about 10 000 Hz can be measured. The standard heterogeneous rate constants k_{et}^0 for the different systems are summarized in Tables 1−3.

In Figure 2, the measured heterogeneous rate constant is plotted as a function of the methylene number of the tethering group for the different SAMs studied here and for the −COOH terminated SAMs; see Niki.[4] At large electrode−reactant separations, the pyridine terminated alkanes and the COOH terminated SAMs display an exponential dependence on the charge-transfer distance (see eqs 1 and 3) with a decay constant of about one per methylene. This decay constant is similar to that found in other tunneling studies with saturated hydrocarbons. This behavior at large distance is a signature for nonadiabatic electron transfer. Both data sets show a plateau region at short donor−acceptor separations; however, the plateau region spans to a larger methylene number for the pyridinal systems. Although the behavior is qualitatively similar for these two systems, the maximum rate constants differ by about a factor of 2 and the rate constants in the pyridine-bound systems are consistently higher than that for the electrostatically bound system.

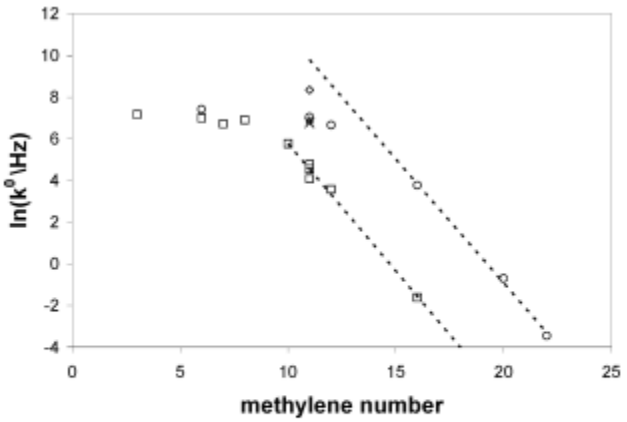

Figure 2. This diagram plots the apparent standard electron-transfer rate constants for the different systems. The data for systems bound through coordination with the heme are represented by a circle for pyridine, × for imidazole, triangle for CN, and diamond for terthiophene. The squares are the data for electrostatic adsorption on COOH. The dashed lines are fits to the nonadiabatic model at a large layer thickness.

An important caveat in using voltammetric peak shifts to obtain rate constants is the presence of *iR* drop in the solution. At faster voltage scan rates the current is higher so that the voltage drop associated with the solution resistance increases. The importance of this effect was evaluated by studying the voltammetry for cytochrome *c* linked to the electrode by way of a pyridine terminated tether of six methylene groups. Of the alkane tethered structures, this system would be expected to show the largest *iR* artifact. A 10-fold increase in the phosphate buffer concentration (the ionic strength) causes a 10% increase in the measured rate constant (data are provided in thesupplemental information). Whether this dependence represents the effect of *iR* drop or change in the protein's electron-transfer rate with ionic strength is currently under study. Even if this change represents the effect of *iR* drop, it represents a minor contribution to the experimental rate constant and cannot explain the weak distance dependence of the electron-transfer rate between six methylene and twelve methylene thick films (see Table 1).

Table 1. Rate Constant Data for Cytochrome *c* Immobilized on Different Mixed SAMs[a]

system	k^o (Hz)	E^o (mV)	no. of trials	system	k^o (Hz)	E^o (mV)	no. of trials
C6py/C5	1580	−175	6	C11CN/C8	1000	−415	2
C11py/C10	1150	−168	14	C11Im/C8	860	−346	4
C12py/C11	785	−172	4	Terpy/C7	4200	−188	2
C16py/C15	52	−158	12				
C20py/C19	0.50	−156	3				
C22py/C20	0.032	−145	2				

[a] In each case, the diluent SAM is an alkanethiol and the measurement is made in aqueous buffer. The data are the average of experimental results obtained on different days with different electrode preparations.

Figure 2 also shows new data on the cytochrome *c* adsorbed through three other tethers in the region of the plateau. In two of these systems, the C11 tether is retained, but the receptor group has been modified from a pyridine to an imidazole and from a pyridine to a nitrile unit. These headgroups cause a quite different apparent redox potential but have a minor effect on the standard electron-transfer rate constant. The shift in the apparent redox potential is consistent with solution studies of cytochrome *c*'s redox potential shift when it binds small ligands. In particular, the immobilized cytochrome *c* studies give −172 mV for the pyridine headgroup, whereas a cytochrome *c* solution with pyridine added has a −294 mV shift.[1a,16a] The imidazole tether causes an apparent redox potential of −346 mV, and the nitrile causes −415 mV, which should be compared to −426 mV and −665 mV for cytochrome *c* solutions containing imidazole and cyanide, respectively.[1a,16b,c] The addition of an exogenous ligand to the solution may cause a conformational change in the protein that might contribute to the redox potential shift, or it may ligate to the heme and cause a shift in the redox potential. A recent study by Fan et al.[16a]distinguishes these two contributions for the case of pyridine and finds that the heme bound pyridine has a redox potential of −161 mV and that the larger negative redox potential of −294 mV should be associated with a non-native protein conformation. Their findings corroborate the view of cytochrome *c* adsorption that is illustrated in Figure 1, in which the cytochrome *c* binds to the pyridine in a nativelike conformation rather than a denatured form. Despite these large changes in the apparent redox potentials, the standard electron-transfer rate constants for the three C11 systems lie within 30% of each other (see Table 1). The other tether is a terthiophene oligomer with a pyridinal head unit. It displays an apparent redox potential that is similar to that found for the alkylpyridine systems, but the rate constant shows a factor of 4 increase (see Table 1), demonstrating the importance of tether composition on the electron-transfer rate.

Figure 3 and Table 2 present the dependence of k_{et}^0 on the solution viscosity, varied by the addition of glucose, for the C6Py, C11Py, and C16Py SAM systems. Fits of the data to the power law form of eq 6 gives γ values of 0.58 for C6Py, 0.28 for C11Py, and ∼0 for C16Py. The dependence on the viscosity correlates with the chain length of the alkane linker. The viscosity dependence is seen in the plateau region of the distance dependence, whereas the rate constant is independent of the viscosity in the large distance regime. The viscosity independence of the rate constant for the C16Py system is consistent with the nonadiabatic mechanism being operative in this regime and demonstrates that the experimental procedure for changing the viscosity is not causing some other change in the protein or its adsorbed state. The "maximal" value of $\gamma \approx 0.58$ found for the plateau region is typical for viscosity dependent protein processes and small molecule reactions.[17] Although the rate constants for C11Py and C6Py are similar, the viscosity

dependence for the C6Py system is significantly steeper than that found for the C11Py system. The observation of a viscosity dependence for the electron-transfer rate constant was observed previously for cytochrome *c* adsorbed electrostatically to carboxylic acid terminated films[4d] and for the $Fe(CN)_6^{3-/4-}$ couple in contact with very thin alkane based monolayer films.[18]Clearly, a viscosity linked process becomes important in the plateau region of the data in Figure 2 and demonstrates a change in the mechanism of the electron-transfer reaction with distance.[19]

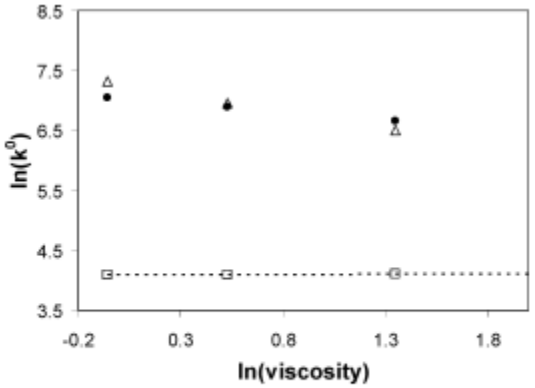

Figure 3. Viscosity dependences of the observed electron-transfer rate constant are shown for three different alkanethiol chain lengths: the triangles are C6, the circles are c11, and the squares are C16. The dashed line has zero slope.

Table 2. Rate Constants of Immobilized Cytochrome *c* for Different Solution Viscosities[a]

	$\eta = 0.98$ cP		$\eta = 1.76$ cP		$\eta = 3.88$ cP	
system	no. of runs	k° (Hz)	no. of runs	k° (Hz)	no. of runs	k° (Hz)
C6py/C5	3	1512	4	1050	3	670
C11py/C10	2	1155	5	990	4	780
C16py/C15	2	60	2	60	2	61

[a] Data are only obtained from the viscosity measurement, which may not be identical to the average data of all measurements, provided in Table 1.

Table 3 provides data that displays a shift in the electron-transfer rate constant for cytochrome *c*when it has been exposed to heavy water.[20] These experiments show that long time exposure (ca. 30 min or more) of the protein to D_2O changes the observed electron-transfer rate constant in the plateau region of Figure 2. If a C11Py/C10 coated electrode is placed in a D_2O buffer solution containing cytochrome *c* and allowed to incubate to form the adsorbed state of the protein, the measured standard electron-transfer rate constant decreases by 30%. This decrease is independent of whether the measurement in the electrochemical cell occurs with H_2O buffer or D_2O buffer. The typical time that the electrode is in the electrochemical cell is less than 10 minutes. These results suggest that water present in the protein or exchangeable protons act to modulate the electron-transfer rate constant in the plateau region. A deuterium isotope effect was also observed by Murgida and Hildebrandt.[21] In contrast, the C16Py/C15 coated electrodes do not display a dependence on D_2O versus H_2O and demonstrate that the modification of the "normal" buffer solution with D_2O does not impact the adsorbed state of the protein.

Table 3. D_2O Dependence of the Rate Constant Data for Immobilized Cytochrome *c*[a]

C11py/C10			C16py/C15		
cell	incubant	k^0 (Hz)	cell	incubant	k^0 (Hz)
H_2O	H_2O	1140	H_2O	H_2O	58
D_2O	H_2O	1100	D_2O	H_2O	
H_2O	D_2O	890	H_2O	D_2O	
D_2O	D_2O	879	D_2O	D_2O	55

[a] Data are only obtained from the isotopic measurements and may not be identical to the average data of all measurements, provided in Table 1.

The results that are presented and summarized here cannot be explained in terms of the nonadiabatic electron-transfer model (eqs 1 and 2) over the whole range of systems. For methylene chains longer than dodecane, the standard electron-transfer rate constant declines exponentially with increasing alkane chain length, does not display a viscosity dependence, and does not change with the use of D_2O buffer. These observations are consistent with the nonadiabatic electron-transfer mechanism. Further, they demonstrate that the method for changing the viscosity and the use of D_2O do not change the adsorption state of the protein. Although the electron-transfer rate constant is well described by the nonadiabatic model at large distances, the reaction mechanism must change for shorter distances because the rate constant is no longer decaying exponentially with distance, displays a viscosity dependence, and depends on the use of D_2O versus H_2O. The nature of the reaction mechanism at short distances and the thickness at which the mechanism changes are discussed below.

4. Discussion

Tunneling Mechanism at Large *n* and the Role of Binding Mode. From Figure 2, one can see that at large electrode−cytochrome *c* separations the data for SAM films that are terminated with pyridinal moieties show a trend similar to that of the −COOH terminated films, but the onset of the exponential decline occurs at larger film thicknesses (ca. 12 methylenes) for the pyridinal case. The steepness of the decline is similar for the two systems, 1.19 per CH_2 for the pyridinal SAMs and 1.22 per CH_2 for the COOH SAMs, and agrees with the fall off found for tunneling through saturated hydrocarbons.[8] The shift between the two cases can be understood by considering the different binding modes of cytochrome on the two film types. The COOH terminated groups electrostatically bind the cytochrome by its lysine groups[4] and the pyridine terminated alkanethiols bind through ligation with the heme group.[22] Inspection of Figure 2 shows that a shift of the COOH rate constants by about four methylene groups to the right would cause a good correspondence between the two data sets.

The reasonableness of such a distance shift can be probed by estimating the physical distance between the electrode surface and the heme unit of the protein in the two cases. Consider the pyridine unit to coordinate at the heme and assume it contributes little to the effective charge-transfer distance because of its π-conjugated nature.[23] The "effective" donor−acceptor separation *d* between the metal surface and the heme, upon the variation of the SAM thickness, can be estimated according to

$$d = 1.90 + 1.12n \text{ (Å)} \qquad (7)$$

where *n* is the number of methylenes in the alkane chain and 1.90 Å accounts for the S atom radius of the thiol.[24] A similar analysis for cytochrome *c* adsorbed on the COOH terminated films requires that the tunneling pathway from the outer layer of the SAM through the protein exterior and into the heme unit be identified. Because of the possibility that the cytochrome can have a range of orientation, one should more formally consider a distance distribution; however, work by Niki[25] implies that the electron tunneling occurs mostly through the lysine 13 which lies near the heme unit. Using the cytochrome *c* crystal structure, one can estimate a physical "through-space" distance of 5.8 Å from the lysine to the heme and a "through-bond" distance of about 20 Å. These considerations of the actual physical distance between the electrode and the heme justify the use of a distance shift to bring the two data sets into correspondence.

Figure 5 presents the dependence of the heterogeneous rate constant for the pyridinal systems as a function of the charge-transfer distance, estimated through eq 7, and for the COOH systems with a 5 Å shift to account for an extra "effective tunneling distance" from the SAM edge through the protein matrix. The good agreement between the two data sets suggests that differences in the electron-transfer rate that is observed can be "corrected" by accounting for differences in the electron-transfer distance. Although it is enticing to attribute this difference to the physical distance of the heme from the electrode in the two situations, this may not be the most accurate description. Rather, differences in the electronic coupling between the heme and the electrode for the two situations, arising from differences in the tunneling pathways, will contribute to the "effective" donor−acceptor separation.

Friction Control versus Conformational Gating. Previous workers[4d,25] have explained the distance independent behavior of the charge-transfer rate constant in the plateau region, for the case of −COOH terminated SAMs, as resulting from a change in the rate-determining step. In particular, the charge transfer occurs by the nonadiabatic (tunneling) mechanism and is gated by a conformational rearrangement to a precursor state that is electroactive. This mechanism is similar to the conformationally gated mechanism that has been used to describe electron-transfer processes involving a range of processes with cytochrome *c*'s.[3b,26] For the COOH terminated SAMs, this may correspond to the diffusive tumbling of the cytochrome *c* on the surface to an orientation in which the protein's heme is closest to the surface and electron transfer occurs rapidly. Such a scenario is not consistent with the data for the pyridine terminated chains, which show a similar distance dependence but do not involve reorientation of the protein on the SAM surface.

A number of results do not support simple conformational gating of the heterogeneous electron transfer on SAM coated Au electrodes. First, the electrochemical data, ac impedance and cyclic voltammetry, indicate a simple charge-transfer step. For example, the peak potential's shift with voltage scan rate and symmetry of the oxidation and reduction waves suggest a simple electrochemical reaction, rather than a mechanism involving a preequilibrium. Second, the observation of similar limiting values of rate constants for the different monolayer films, which have two very different binding modes of cytochrome *c*, suggests that the electron transfer is not preceded by the large-scale protein−SAM structural rearrangement (conformationally gated). Third, the dependence of the electron-transfer rate constant on the amount of D_2O in the adsorbed protein, rather than D_2O in the solution, is not consistent with large-scale motion of the

protein on the surface of the film. Fourth, the larger rate constant that is found for the conjugated terthiophene tether cannot be explained by a conformational gating mechanism. These observations indicate that conformational gating is not controlling the electron-transfer rate constant for the pyridine terminated SAMs, but it does not discount this mechanism for the COOH terminated SAMs nor does it discount small amplitude conformational changes that may be linked to the electron-transfer coordinate.

An adiabatic charge-transfer mechanism for the charge-transfer kinetics in the plateau region is consistent with the findings. In particular, the viscosity dependence of the rate and the D_2O effects can be understood through consideration of frictional coupling in the adiabatic mechanism, whereas the higher electron-transfer rate for the conjugated linker can be rationalized through the effect of the electronic coupling on the activation barrier for the reaction (eq 5). The increase in rate constant for the conjugated system supports the adiabatic mechanism over the conformationally gated mechanism. A critical test for distinguishing between the two mechanisms is to determine the free energy dependence of the reaction rate constant. For an adiabatic electron-transfer mechanism, the rate constant should display a Marcus bell-shaped dependence on free energy, whereas a conformationally gated mechanism should not.[1a,3a,27] In lieu of such experiments, electron-transfer rate constants for many different cytochrome *c* systems were obtained from the literature and analyzed as a function of free energy.

Comparison of Homogeneous and Electrochemical Kinetics. Figure 4 plots electron-transfer rate constants as a function of ΔG_0 for many different systems involving cytochrome *c* (including the "limiting" electrochemical value, k_{el}^0). These data include "unimolecular" systems,[2] in which a redox center is covalently attached to the cytochrome *c*, and bimolecular systems.[3] Because they have a well-defined metal-to-metal separation distance, the unimolecular systems can be compared with the electrochemical data in more detail (vide infra). An analysis of this sort presumes that the electron-transfer rate is determined primarily by the Franck−Condon factors (free energy and reorganization energy) rather than the electronic coupling and that the reorganization energy does not change too dramatically between the different systems. Despite the drastic nature of these assumptions, the rate constants fall surprisingly well on a bell-shaped curve.

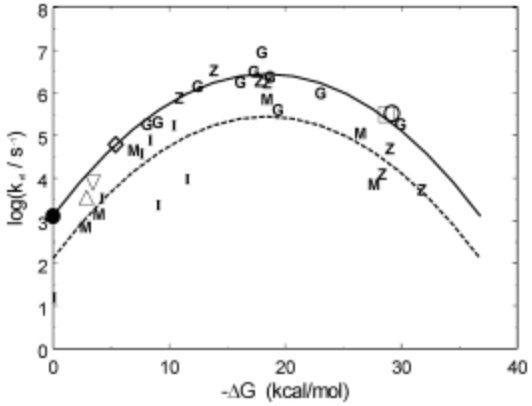

Figure 4. This Marcus plot shows the free energy dependence of cytochrome *c*'s electron-transfer rate constant from a number of different studies, mostly homogeneous solution; the data are from Gray et al. [G][2d] for Ru-modified cytochrome *c*; Zhou et al. [Z][2b] for cytochrome *c*/uroporphyrin complexes; McLendon[3a] for interprotein system cytochrome *c*/cytochrome b_5 [M]; and Isied et al[2e] for Ru-modified cytochrome *c* [1]. The open symbols (◇[3c], ▽[3f], □[3b], △[3d], ○[3e]) correspond to rate constants that exhibit a dependence on the external solution viscosity. The filled circle shows the electrochemical electron-transfer rate at short distances (plateau region), which also displays a viscosity dependence.[4d] The solid curve shows the free energy dependence expected from the Marcus model, and the dashed curve is the same model shifted down by a factor of 10.

The solid curve drawn in Figure 4 is generated by fitting the rate data for a series of ruthenium-modified cytochrome *c*'s.[2] This data set (G) was used because of the range of free energies and the well-defined distances between the redox centers. The kinetic data that are plotted with open symbols (cytochrome *c*/P870 in Rb.
Sphaerodis,[3f] cytochrome *c*/Ru(II)bpy,[3b] cytochrome *c*/radical cation in cytochrome *c* peroxidase,[3c] zinc cytochrome *c*/bean plastocyanin,[3d] and cytochrome *c*/fern plastocyanin[3e] complexes) exhibit a dependence on the external solution viscosity. The electrochemical rate data appear to follow this Marcus free energy dependence. The electrochemical rate constant (filled circle) measured at $\Delta G_0 = 0$ shows a 1000-fold reduction from the maximum rate constant but lies on the same curve. This observation suggests that the electrochemical system follows the free energy dependence for electron transfer. The observed free energy dependence of the rate data and the viscosity-sensitive behavior for some of them (Figure 4) indicate that the electron transfer belongs either to the totally adiabatic (friction controlled) or, at least, to the intermediate (or mixed, vide infra) kinetic regimes, rather than corresponding to a conformationally gated mechanism.[27d]

The data in Figure 4 and the general correspondence with the reaction free energy reflects the importance of the activation free energy on the reaction rate constant. The large scatter in the rate data is to be expected, since the data correspond to cytochrome *c* in such different environments. The peak of the curve corresponds to the reaction free energy magnitude that matches the reorganization energy so that the reaction rate is at a maximum. The dashed line in the figure was obtained by shifting the solid curve down by an order of magnitude. The data show that the free energy and reorganization energy determine the rate constant to within an order of magnitude or so. This data analysis generates a reorganization energy for the cytochrome *c* of 0.8 eV. Although the reorganization energy depends on both partners in a redox reaction, these data suggest that the protein dominates the contribution and is fairly consistent between systems. For

the electrochemical studies, the kinetic data probe the reorganization energy through the dependence of k_{et} on ΔG_0 (i.e., the overpotential $e\xi$) by way of eq 8,

$$k_{et} \propto \int_{-\infty}^{\infty} f(\epsilon) \exp\left[-\frac{(e\xi + \epsilon_F - \epsilon \pm \lambda)^2}{4\lambda RT}\right] d\epsilon \qquad (8)$$

where $f(\varepsilon)$ is the Fermi−Dirac distribution function and ε_F is the Fermi energy.[8] When $|\Delta G_0| \leq \lambda$, the electrochemical data coincides with the solid curve in Figure 4.[28a]

A number of experimental and theoretical studies[28,29] report the reorganization energy of cytochrome *c*, and they range in value from 0.8 eV to 0.4 eV for the protein in solution. What portion reflects an intrinsic protein component and what portion arises from the environment or redox partner has been addressed through theoretical studies.[29] These studies find that the inner sphere (heme) contribution to the reorganization energy is about 0.1 eV, the protein's "outer sphere" (interior) contribution is at least 0.45 eV, and the solvent's contribution is about 0.25 eV.[29]The reasonable characterization of the rate data with a single reorganization energy and the theoretical studies imply that the reorganization energy, although the solvent affects it, is primarily determined by the protein environment.

A Unified Model for the Electron Transfer. Theoretical work[30] that accounts for both the tunneling (distance controlled, eq 1) and friction controlled (viscosity dependent, eq 6) charge-transfer mechanisms and a gradual turnover between them is available. Adapting the unified expression for the unimolecular rate constant to an electrode process at ΔG_0, one finds

$$k_{et}^{o} = \frac{|V|^2}{\hbar} \frac{\rho_m}{1+g} \sqrt{\frac{\pi^3 RT}{\lambda_o}} \exp(-\Delta G_a/RT) \qquad (9)$$

in which ρ_m is the density of electronic states in the electrode and the adiabaticity parameter g is given by

$$g = \frac{\pi^3 RT |V|^2 \rho_m \tau_{eff}}{\hbar \lambda_o} \qquad (10)$$

g acts as a control parameter; the reaction mechanism is nonadiabatic when $g \ll 1$, yielding the equation

$$k_{NA}^{o} = \frac{|V|^2}{\hbar} \rho_m \sqrt{\frac{\pi^3 RT}{\lambda_o}} \exp(-\Delta G_a/RT) \qquad (11)$$

For long-range electron transfer in biological systems, the weak coupling or nonadiabatic regime, in which the process is viewed as a tunneling ("quantum friction") mechanism, is used for both homogeneous[2] and heterogeneous[4] electron-transfer reactions. The mechanism is adiabatic when $g \gg 1$, yielding the expression

$$k_A^o = \frac{1}{\tau_{eff}}\sqrt{\frac{\lambda_o}{\pi^3 RT}}\exp(-\Delta G_a/RT) \qquad (12)$$

where the characteristic time τ_{eff} is related to relaxation processes of the solvent molecules, protein interior, and so forth. In the approximation of a dielectric continuum and a Debye-type dielectric response, one finds that

$$\tau_{eff} \approx \tau_L = \left(\frac{\epsilon_\infty}{\epsilon_s}\right)\frac{3\eta V_m}{RT} \qquad (13)$$

where τ_L is the longitudinal relaxation time of the solvent polarization and η is the solvent shear viscosity.[30a] The other parameters are the molar volume V_m, the static dielectric constant ε_S, and the high-frequency dielectric constant ε_∞. For the case of more complex environments, τ_{eff} might be associated with some conformational or molecular rearrangement that is coupled to the electron transfer. The strong coupling, or adiabatic regime, is often used to describe short-range electron transfer and is viewed as solvent controlled (overdamped) motion in a single electronic state (sometimes called the "friction mechanism"). The experimental signature for electron transfer in this regime is a friction (or viscosity) dependent rate constant, often characterized by the power law form, eq 6, as mentioned in the introductory section. To summarize, the nonadiabatic electron-transfer mechanism displays an exponential distance dependence and viscosity independence, whereas the adiabatic mechanism displays a viscosity dependence but no exponential distance dependence.

Equation 10 reveals that the electron-transfer mechanism depends on the value of $|V|^2$ compared to the other parameters τ_{eff} and λ_o. Recent work studying the electron exchange of the $Fe(CN)_6^{3-/4-}$ redox couple with alkanethiol coated gold electrodes observed the transition from the adiabatic to nonadiabatic regime with the increasing thickness of the electron tunneling barrier.[18]For this redox couple the transition between the nonadiabatic and adiabatic mechanisms occurred at an electron exchange distance of ca. 8−9 Å (distance for g = 1) and a relaxation time of about 50 ps in an 11 cP aqueous electrolyte solution; of course, the actual value depends on the particulars of the system under study. For electron-transfer processes in highly structured media with long relaxation times τ_{eff} and small reorganization energies λ_o, for example, a protein, the transition from the adiabatic regime to the nonadiabatic regime should occur at much smaller values of $|V|$, which may correspond to relatively long distances.

The distance dependence of the electron-transfer rate constant for cytochrome *c* can be quantitatively compared to eq 9. To perform the analysis for a wider range of data (the unimolecular data of Gray[2] and the electrochemical data[4]), the observed electron-transfer rate constants were converted to their maximum (optimal) values k_{max} by rearrangement of eq 9

$$k_{max} \equiv k_{et}^o \exp(\Delta G_a/RT) = \frac{|V|^2}{\hbar}\frac{\rho_m}{1+g}\sqrt{\frac{\pi^3 RT}{\lambda_o}} \qquad (14)$$

This transformation removes the activation barrier from the considerations and allows the dynamical part of the rate constant to be studied. This procedure requires accurate knowledge of

the activation energy, however. The data in Figure 5 show this transformation if the reorganization energy 0.8 eV, as suggested by the Figure 4, is used for the three data sets. The value of k_{max} is sensitive to uncertainty in the reorganization energy that is used; for example, changing the reorganization energy to 0.6 eV reduces the value of k_{max} in Figure 5 by a factor of 7.

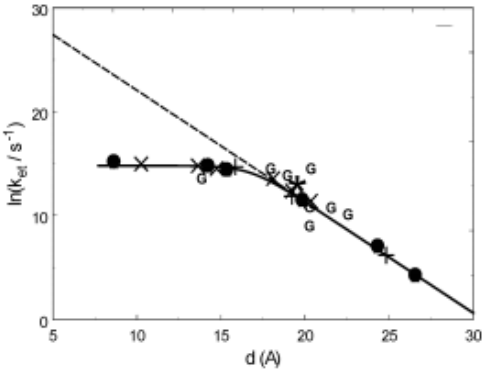

Figure 5. Maximum electron-transfer rate constants (eq 14) for cytochrome *c* from Figure 2 are plotted as a function of the electron-transfer distance. A constant distance of 5 Å has been added to the electrochemical data on the carboxylic acid terminated films (×, Niki et al.[4c,d]; +, Bowden et al.[4a,b]; *, this work) so that they coincide with the data on pyridine terminated layers (●) and the data of Gray et al. (G).[2c] The solid black curves are fits to eq 14, and the dashed line shows the predicted nonadiabatic electron-transfer rate constant at a shorter distance.

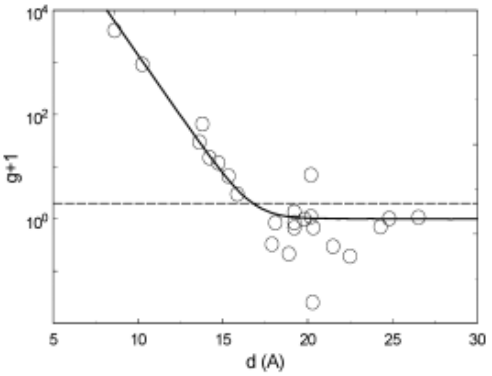

Figure 6. The logarithm of the ratio of the calculated nonadiabatic (simple linear extrapolation, Figure 5) to the experimental rate constants, $k_{NA}/k_{EXP} = 1 + g$, is plotted versus the effective charge transfer distance for the cytochrome *c* systems. The solid curve represents the best fit, eqs 9 and 10. The horizontal dashed line shows the case of $g = 1$.

Given this assumption about the reorganization energy, Figure 5 plots the distance dependence of k_{max} for the two electrochemical systems and the homogeneous studies as a function of the distance between the redox active heme of the cytochrome and the electron donor, gold electrode and ruthenium moiety. The •'s correspond to the rate constants of the pyridine terminated SAMs and the G's correspond to the unimolecular rate constant data of Gray.[2] The data for the COOH terminated SAMs (×, *, +) did not show a good correspondence with the other two data sets unless the electron-transfer distance was increased by 5 Å, as discussed with regard to eq 7. This shift, to account for an extra “effective tunneling distance”, provides excellent correspondence among the three data sets. The solid black curve in Figure 5 shows a fit to eq 14, which describes the transition between electron-transfer regimes. The dashed line corresponds to an extrapolation of the nonadiabatic rate constant back toward short distances. Although the good correspondence between eq 14 and the data is compelling, it is important to assess the values of the parameters in the model and their reasonableness.

Fitting of the rate constant data in the different regimes allows the adiabaticity parameter *g* to be evaluated. By fitting the electron-transfer rate constants at large distances to the nonadiabatic model, one can define the parameters that describe the nonadiabatic rate. Using a reorganization energy of 0.8 eV and a density of states for the Au electrode[8b] of 0.28 eV^{-1}, one finds an electronic coupling between the Au electrode and cytochrome *c* of 0.17 cm^{-1} at 17 Å. This coupling magnitude and the measured decay length at a long distance, β of 1.07/Å, can be used to predict what the nonadiabatic rate constant would be at shorter distances. In the plateau region of the kinetics, the fit of the data to the adiabatic model requires that the characteristic relaxation time for the protein's polarization response τ_{eff} be 188 ns. This relaxation time is unusually long for a pure liquid solvent response; however, the protein provides a highly structured solvation

environment, and its polarization relaxation should be slower than that of a simple redox system. Note that a change in the magnitude of k_{max}, arising from uncertainty in the reorganization energy, causes a corresponding change in the relaxation time, but it still remains in the time range of hundreds of nanoseconds. Using eq 14, it is then possible to extract the adiabaticity parameter *g*, which controls the transition between regimes. Figure 6 plots 1 + *g* as a function of distance between the redox sites, that is, the heme and the electrode. The horizontal dashed line shows the location of $g = 1$ and marks the transition between regimes, which occurs between 16 and 17 Å. At large distances, *g* goes asymptotically to zero, and at short distances, it increases exponentially. This analysis requires that the electron-transfer mechanism for cytochrome *c* lie in the strong to intermediate regimes at distances up to 17 Å.

Is such a long polarization relaxation time reasonable? Most direct studies of solvation relaxation times have been performed for small organic molecules in neat polar liquids and have rapidrelaxation times, ranging from a few hundred femtoseconds in acetonitrile to a few hundred picoseconds in *n*-decanol.[31a] In more highly structured solvents, such as 1,3-butanediol and alcohol glasses, the solvation times can be in the regime of nanoseconds.[31] However, relaxation times as low as 10^{-4}−10^{-8} s have been reported for the myoglobin heme pocket, even at room temperature (see refs 32 and 33). Compared to these values, the 188 ns time required by this analysis seems reasonable for the protein interior. For this time scale to be physically reasonable, the polarization response must involve some sort of quasi-diffusional conformational motion in the protein. It is worth mentioning that this 188 ns time lies close to the low-frequency edge for the actual conformation fluctuation spectrum of native cytochrome *c* and near the upper bound for helix−coil transitions of peptide chains.[34] Other conformational changes that accompany the redox reaction,[29,35,36] including a shift of interglobular “catalytic water”,[36] may contribute to the frictional coupling. Alternatively, it may be that proton transfer is linked to the electron-transfer coordinate.[21]Certainly, the D_2O studies would be consistent with a reaction coordinate that involved water(s) in the protein or proton transfer. The results are also consistent with the finding that electron transfer in cytochrome *c* can be used to trigger the folding/unfolding of the protein, and they suggest that this process is associated with a conformational change in the protein that modifies the polarization along the redox reaction coordinate. The unified model, represented by eq 14, is able to describe the distance dependent rate constants with an effective polarization relaxation time of 150−200 ns.

Included in this study is the linking of the protein to the gold electrode through a terthiophene tether that is terminated with a pyridine unit. In this case, a substantial increase of the rate constant is observed, almost 4-fold, while the formal redox potential remains the same as for the alkane analogue. In the adiabatic charge transfer picture, this increase can be understood as a decrease in the activation barrier to the electron transfer that arises from an increased electronic coupling strength (see eq 5). This observation is not consistent with a conformational gating model, since the pyridine group, which is the portion of the tether that interacts directly with the protein, is the same for the alkane and terthiophene tethers. Using the same parameters for the electron transfer as described previously, these data indicate that the electronic coupling must change by 0.03 eV (ca. 250 cm^{-1}) for a 4-fold increase in the rate constant. Given the small value for the electronic coupling through the alkane tether, one can assign the change in electronic coupling strength to the terthiophene-linked protein. By comparison with other studies of conjugated molecular wires, one estimates an electronic coupling for a conjugated, $n = 12$ tether

to be 100−1000 times larger than that for an equivalent length alkane chain.[23] This increase is in agreement with the value found below for the alkane tethered pyridine case (vide infra). Within the nonadiabatic (tunneling) picture, this coupling corresponds to a 10^4−10^6 increase in the charge transfer rate constant (see eq 1), which is clearly not found. This rate constant for the terthiophene linker can be rationalized by a rate-determining charge-transfer step that operates through an adiabatic mechanism, rather than a nonadiabatic mechanism.

Comparison with Other Redox Protein Systems. Only a few reports plot the biological electron-transfer data for comparable donor−acceptor distances below 10−15 Å, where one expects a transition from the nonadiabatic to adiabatic mechanism. These studies include primary electron-transfer steps in photosynthetic reaction centers[32,37] and recent data on azurin that is adsorbed to a SAM coated gold electrode.[38] The azurin data display behavior similar to that found in cytochrome *c*, a plateau region for thin SAM films. The authors of that report restricted their discussion to the gated mechanism, which is not appropriate for the current system, for the reasons outlined previously. Whether the electron transfer involving cytochrome *c* in the reaction centers occurs by the adiabatic mechanism is not clear. Indeed, these natural systems may display a large degree of inhomogeneity (see refs 32 and 37). The kinetics for some of the electron-transfer processes is clearly not exponential, and this behavior has been explained by a broad distribution of nonadiabatic electron-transfer rates and by a mixed adiabatic/nonadiabatic model.[32,37] It may be that intramolecular quantum degrees of freedom contribute significantly to the reorganization energy for some of the primary electron-transfer steps in the photosynthetic reaction center,[37] and this could modify the onset of the nonadiabatic to adiabatic mechanism change. In terms of the classical model used previously, the quantum degrees of freedom act to renormalize the electronic matrix element $|V|$ and shift the onset of the frictional regime to smaller donor−acceptor distances.[6] Such a condition may be crucial for the primary steps in photosynthesis and might result from special evolutionary forces. A manifestation of kinetically coupled quantum modes, a significant inner sphere reorganization contribution, causes a distortion of the bell-shaped free energy plot, Figure 5, on the side of highly negative free energy gaps.[6] No such distortion is evident in Figure 5 and indicates a minor role for high-frequency vibrational modes in the cytochrome electron transfer, in agreement with the results of ref 29.

Conclusions

Conventional electrochemical techniques were applied to the electron transfer of cytochrome *c* protein immobilized on the surface of SAM modified electrodes. Chemical control of the adsorption allowed the accurate determination of heterogeneous unimolecular rate constants for the electron exchange between the SAM-modified metal electrode and the cytochrome *c*. This approach allowed the charge-transfer rate constant's dependence on distance, solution viscosity, and other parameters to be studied in detail. The data display a change in the electron-transfer mechanism with the distance from the electrode and the rate constant's dependence on viscosity, and the chemical composition of the SAM was studied in each regime.

Analysis of these and published kinetic data for cytochrome *c* with a unified model for cytochrome *c*'s redox kinetics is presented. Although this analysis ignores detailed differences between the heme environment in the data sets, it provides a good representation of the rate constant's distance dependence and suggests that the electron transfer occurs very close to, or in,

the intermediate (still viscosity sensitive) regime at physiologically significant distances, ca. 17 Å. This explanation requires that the electron-transfer event be coupled to a polarization response of the medium (the protein interior and its environment, including the protein/water boundary hydrogen-bonded network) with an unusually long characteristic relaxation time of a few hundred nanoseconds. The detailed features of this response and its molecular character remain unclear, but it may involve a conformational motion that is linked to the polarization response along the electron-transfer reaction coordinate. Under such conditions, the transformation from adiabatic to nonadiabatic regimes could occur at large electron-transfer distances, ca. 17 Å or more.

What advantage arises from an adiabatic (friction controlled) electron-transfer mechanism for cytochrome *c*? It may be that the multiple functions of cytochrome *c* require external regulatory tools of mechanism switching that can be implemented through specific protein−protein interactions. In particular, because the reaction occurs in the frictional or intermediate electron-transfer regime, the strong dependence of the rate constant on the donor−acceptor distance is prevented and the polarization response acts as a "throttle" for the reaction. Whether these findings arise from the particular construction of cytochrome *c* and are associated with its special role as a redox protein in living cells or whether it is more generally operative in biological systems remains an open question.

Acknowledgment

D.E.K. and D.H.W. are grateful to the National Research Council, Office of International Affairs, for financial support in the framework of Twinning Program Grant, 1999-2000. D.E.K. also kindly acknowledges the Collaborative Linkage Grant (PST.CLG 975701) from the North Atlantic Treaty Organization. D.H.W. acknowledges partial support from the National Science Foundation, CHE-0111435, and the U.S.−Israel Binational Science Foundation.

Supporting Information Available

Supporting Information, which show measurements of the electron-transfer rate constant as a function of ionic strength, is available. This material is available free of charge via the Internet at http://pubs.acs.org.

References

(a) Fedurco, M. *Coord. Chem. Rev.* **2000**, *209*, 263. (b) Scott, R. A. In *Cytochrome C: A Multidisciplinary Approach*; Scott, R. A., Mauk, A. G., Eds.; University Science Books: Sausalito, CA, 1996; p 515.

(a) Meade, T. J.; Gray, H. B.; Winkler, J. R. *J. Am. Chem. Soc.* **1989**, *111*, 4353. (b) Zhou, J. S.; Rodgers, M. A. J. *J. Am. Chem. Soc.* **1991**, *113*, 7728. (c) Casimiro, D. R.; Richards, J. H.; Winkler, J. R.; Gray, H B. *J. Phys. Chem.* **1993**, *97*, 13073. (d) Mines, G. A.; Bjerrum, M. J.; Hill, M. G.; Casimiro, D. R.; Chang, I.-J.; Winkler, J. R.; Gray, H. B. *J. Am. Chem. Soc.* **1961**, *118*, 1961. (e) Luo, J.; Reddy, K. B.; Salameh, A. S.; Wishart, J. F.; Isied, S. S. *Inorg. Chem.* **2000**, *39*, 2321.

(a) McLendon, G. *Acc. Chem. Res.* **1988**, *21*, 160. (b) Harris, M. R.; Davis, D. J.; Durham, B.; Millett, F. *Biochim. Biophys. Acta* **1997**, *1319*, 147. (c) Mei, H.; Wang, K.; Peffer, N.; Weatherly, G.; Cohen, D. S.; Miller, M.; Pielak, G.; Durham, B.; Millett, F. *Biochemistry***1999**, *38*, 6846.(d) Ivković-Jensen, M. M.; Kostić, N. M. *Biochemistry* **1997**, *36*, 8135.(e) Pletneva, E. V.; Fulton, D. B.; Kohzuma, T.; Kostić, N. M. *J. Am. Chem. Soc.* **2000**, *122*, 1034.(f) Overfield, R. E.; Wraight, C. A.; DeVault, D. *FEBS Lett.***1979**, *105*, 137.

(a) Tarlow, M. J.; Bowden, F. F. *Am. Chem. Soc.* **1991**, *113*, 1847. (b) Song, S.; Clark, R. A.; Bowden, F. F.; Tarlow, M. J. *J. Phys. Chem.* **1993**, *97*, 6564.(c) Feng, Z. Q.; Imabayashi, S.; Kakuichi, T.; Niki, K. *J. Chem. Soc., Faraday Trans.* **1997**, *93*, 1367. (d) Avila, A.; Gregory, B. W.; Niki, K.; Cotton, T. M. *J. Phys. Chem. B* **2000**, *104*, 2759.

Wei, J.; Liu, H.; Khoshtariya, D. E.; Yamamoto, H.; Dick, A.; Waldeck, D. H. *Angew. Chem., Int. Ed.* **2002**,*41*, 4700.

(a) Barbara, P. F.; Meyer, T. J.; Ratner, M. A. *J. Phys. Chem.* **1996**, *100*, 13148. (b) Curry, W. B.; Grabe, M. D.; Kurnikov, I. V.; Skourtis, S. S.; Beratan, D. N.; Regan, J. J.; Aquino, A. J. A.; Beroza, P.; Onuchic, J. N. *J. Bioenerg. Biomembr.* **1995**, *27*, 285. (c) Closs, G. L.; Miller, J. R. *Science* **1998**, *240*, 440.

Beratan, D. N.; Betts, J. N.; Onuchic, J. N. *Science* **1991**, *252*, 1285.

(a) Finklea, H. O. In *Electroanalytical Chemistry*; Bard, A. J., Rubinstein, I., Eds.; Marcel Dekker: New York, 1996; Vol. 19, p 109. (b) Chidsey, C. E. D. *Science* **1991**, *251*, 919. (c) Miller, C. J. In *Physical Methods in Electrochemistry*; Rubinstein, I., Ed. Wiley: New York, 1995; p 27.

Kramers, H. A. *Physica* **1940**, *7*, 284. (a) Weaver, M. J.; McManis, G. E. *Acc. Chem. Res*. **1990**, *23*, 294. b) Weaver, M. J. *Chem. Rev*. **1992**, *92*, 463. (c) Fawcett, W. R.; Opallo, M. *Angew. Chem., Int. Ed. Engl*. **1994**, *33*, 2131. (d) Williams, M. E.; Crooker, J. C.; Pyati, R.; Lyons, L. J.; Murray, R. W. *J. Am. Chem. Soc*. **1997**, *119*, 10249. (e) Fu, Y.; Cole, A. S.; Swaddle, T. W. *J. Am. Chem. Soc*. **1999**, *121*, 10410. (f) Khoshtariya, D. E.; Dolidze, T. D.; Krulic, D.; Fatouros, N.; Devilliers, D. *J. Phys. Chem. B* **1998**, *102*, 7800.

(a) Wei, J.; Liu, H.; Dick, A. R.; Yamamoto, H.; He, Y.; Waldeck, D. H. *J. Am. Chem. Soc.* **2002**, *124*, 9591. (b) Yamamoto, H.; Liu, H.; Waldeck, D. H. *Chem. Comm.* **2001**, 1032.

Bard, A. J.; Faulkner, L. R. *Electrochemical Methods*; Wiley: New York, 1980.

(a) Hu, J.; Fox, M. *J. Org. Chem*. **1999**, *64*, 4959. (b) Abbotto, A.; Bradamante, S.; Facchetti, A.; Pagani, G. *J. Org. Chem*. **1997**, *62*, 5755.

(a) Edmiston, P. L.; Lee, J. E.; Cheng, S.-S.; Saavedra, S. S. *J. Am. Chem. Soc.* **1997**, *119*, 560. (b) Dick, L. A.; Haes, A. J.; van Duyne, R. P. *J. Phys. Chem. B* **2000**, *104*, 11752.

(a) Napper, A. M.; Liu, H.; Waldeck, D. H. *J. Phys. Chem. B* **2001**, *105*, 7699. (b)Tender, L.; Carter, M. T.; Murray, R. W. *Anal. Chem.* **1994**, *66*, 3173. (c) Weber, K.; Creager, S. E. *Anal. Chem.* **1994**, *66*, 3166. (d) Honeychurch, M. J. *Langmuir* **1999**, *15*, 5158.

(a) Fan, C.; Gillespie, B.; Wang, G.; Heeger, A. J.; Plaxco, K. W. *J. Phys. Chem. B* **2002**, ASAP. (b) Battistuzzi, G.; Borsari, M.; Cowan, J. A.; Ranieri, A.; Sola, M. *J. Am. Chem. Soc.* **2002**, *124*, 5315. (c) Battistuzzi, G.; Borsari, M.; Ranieri, A.; Sola, M. *J. Am. Chem. Soc.* **2002**, *124*, 26.

a) Waldeck, D. H. *Chem. Rev.* **1991**, *91*, 415. (b) Fayer, M. D. *Annu. Rev. Phys.Chem.* **2001**, *52*, 315. (c) Frauenfelder, H.; Wolynes, P. G.; Austin, R. H. *Rev.Mod. Phys.* **1999**, *71*, S419.

Khoshtariya, D. E.; Dolidze, T. D.; Zusman, L. D.; Waldeck, D. H. *J. Phys. Chem. A* **2001**, *105*, 1818.

A viscosity dependent rate constant may occur when the barrier-crossing process has a dissipative nature, experiences frictional coupling with the medium (solvent). For the case of "full" solute−solvent coupling, $\gamma \rightarrow 1$, the Smoluchowski limit. Deviation from this limit may be caused by weak, or intermediate, solute−solvent coupling or a change toward a weaker electronic coupling, as discussed later. Some of these data were reported in ref 5.

Murgida, D.; Hildebrandt, P. *J. Am. Chem. Soc.* **2001**, *123*, 4062.

Murgida, D.; Hildebrandt, P.; Liu, H.; Wei, J.; Waldeck, D. H., in preparation.

(a) Sikes, H. D.; Smalley, J. F.; Dudek, S. P.; Cook, A. R.; Newton, M. D.; Chidsey, C. E. D.; Feldberg, S. W.*Science* **2001**, *291*, 1519. (b) Creager, S.; Yu, C. J.; Bamdad, C.; O'Connor, S.; Maclean, T.; Lam, E.; Chong, Y.; Olsen, G. T.; Luo, J.; Gozin, M.; Kayyem, J. F. *J. Am. Chem. Soc.* **1999**, *121*, 1059.

Liu, Y.-P.; Newton, M. D. *J. Phys. Chem.* **1994**, *98*, 7162.

Niki, K.; Sprinkle, J. R.; Margoliash, E. *Bioelectrochemistry* **2002**, *55*, 37.

a) Engstrom, G.; Xiao, K. H.; Yu, C. A.; Yu, L.; Durham, B.; Millett, F. *J. Biol. Chem.* **2002**, *277*, 31072. (b) Sharp, R. E.; Chapman, S. K. *Biochim. Biophys. Acta* **1999**, *1432*, 143. (c) Canters, G. W.; Dennison, C. *Biochimie* **1995**, *77*, 506.

(a) McLendon, G.; Pardue, K.; Bak, P. *J. Am. Chem. Soc*. **1987**, *109*, 7540. (b) Graige, M. S.; Feher, G.; Okamura, M. Y. *Proc. Natl. Acad. Sci. U.S.A.* **1998**, *95*, 11679. (c) Davidson, V. *Biochemistry* **2000**, *39*, 4924. (d) Davidson, V. *Acc. Chem. Res*. **2000**, *33*, 87.

(a) Terrettaz, S.; Cheung, J.; Miller, C. J. *J. Am. Chem. Soc.* **1996**, *118*, 7857. (b) Winkler, J. R.; DiBilio, A. J.; Farrow, N. A.; Richards, J. H.; Gray, H. B. *Pure Appl. Chem.* **1999**, *71*, 1753. (c) Legrand, N.; Bondon, A.; Simonneaux, G. *Inorg. Chem.* **1996**, *35*, 1627.

(a) Miyashita, O.; Go, N. *J. Phys. Chem. B* **2000**, *104*, 7516. (b) Sigfridsson, E.; Olsson, M. H. M.; Ryde U. *J. Phys. Chem. B* **2001**, *105*, 5546. (c) Basu, G.; Kitao, A. Kuki, A.; Go, N. *J. Phys.*

Chem. B **1998**, *102*, 2085. (d) Muegge, I.; Qi, P. X.; Wand, A. J.; Chu, Z. T.; Warshel, A. *J. Phys. Chem. B* **1997**, *101*, 825.

(a) Zusman, L. D. *Z. Phys. Chem*. **1994**, *186*, 1. (b) Beratan, D. N.; Onuchic, J. N. *J. Chem. Phys* **1988**, *89*, 6195. (c) Onuchic, J. N.; Beratan, D. N.; Hopfield, J. J. *J. Phys. Chem.* **1986**, *90*, 3707.

(a) Maroncelli, M. *J. Mol. Liq.* **1993**, *57*, 1. (b) Nandi, N.; Bhattacharyya, K.; Bagchi, B.*Chem. Rev.* **2000**, *100*, 2013.

Kotelnikov, A. I.; Ortega, J. M.; Medvedev, E. S.; Psikha, B. L.; Garcia, D.; Mathis, P. *Bioelectrochemistry***2002**, *56*, 3.

(a) Bashkin, J. S.; McLendon, G.; Mukamel, S.; Marohn, J. *J. Phys. Chem.* **1990**, *94*, 4757. (b) Pierce, D. W.; Boxer, S. G. *J. Phys. Chem.* **1992**, *96*, 5560. (c) Beece, D.; Eisenstein, L.; Frauenfelder, H.; Good, D.; Marden, M. C.; Reinisch, L.; Reynolds, A. H.; Sorensen, L. B.; Yue, K. T. *Biochemistry* **1980**, *19*, 5147.

Eaton, W. A.; Munoz, V.; Thompson, P. A.; Henry, E. R.; Hofrichter, J. *Acc. Chem. Res.* **1998**, *21*, 745.

(a) Banci, L.; Bertini, I.; Gray, H. B.; Luchinat, C.; Reddig, T.; Rosato, A.; Turano, P. *Biochemistry* **1997**, *36*, 9867. (b) Qi, P. X.; Beckman, R. A.; Wand, A. J. *Biochemistry* **1996**, *35*, 12275. (c) Moss, D.; Nabedryk, E.; Breton, J.; Mantele, W. *Eur. J. Biochem.* **1990**, *187*, 565. (d) Yuan, X.; Sun, S.; Hawkridge, F. M.; Chlebowski, J. F.; Taniguchi, I. *J. Am. Chem. Soc.* **1990**, *112*, 5380. (e) Cohen, D. S.; Pielak, G. J. *J. Am. Chem. Soc.***1995**, *117*, 1675.

(a) Bertini, I.; Hajieva, P.; Luchinat, C.; Nerinovski, K. *J. Am. Chem. Soc.* **2001**, *123*, 12925. (b) Bertini, I.; Huber, J. G.; Luchinat, C.; Piccioli, M. *J. Magn. Reson.* **2000**, *147*, 1. (c) Qi, P. X.; Urbauer, J. L.; Fuentes, E. J.; Leopold, M. F.; Wand, A. *J. Struct. Biol.* **1994**, *1*, 378. (d) Bertini, I.; Dalvit, C.; Huber, J. G.; Luchinat, C.; Piccioli, M. *FEBS Lett.* **1997**, *415*, 45.

(a) McMahon, B. H.; Müller, J. D.; Wraight, C. A.; Nienhaus, G. Ulrich; *Biophys. J.* **1998**, *74*, 2567. (b) Nonella, M.; Schulten, K. *J. Chem. Phys*. **1991**, *95*, 2059.

(a) Chi, Q.; Zhang, J.; Andersen, J. E. T.; Ulstrup, J. *J. Phys. Chem. B* **2001**, *105*, 4669. (b) Zhang, J.; Chi, Q.; Kuznetsov, A. M.; Hansen, A. G.; Wackerbarth, H.; Christensen, H. E. M.; Andersen, J. E. T.; Ulstrup, J. *J. Phys. Chem. B* **2002**, *106*, 1131.

The Impact of Ionic Strength on the Measured Rate Constant

To address the importance of iR drop on the measured standard heterogeneous rate constant, experiments were performed at a range of solution ionic strengths for the C5/C6-Py system. This system was studied because it had the highest rate constant of the alkyl tethered systems and should be most susceptible to problems with the iR drop artifact. Data were collected for buffer solution concentrations ranging from 20 mM to200 mM. buffer solution and at different viscosities. The data in the graph show the trend in the rate constant with ionic strength in the aqueous buffer solution. The data in the table show the extreme rate constants at three different viscosities.

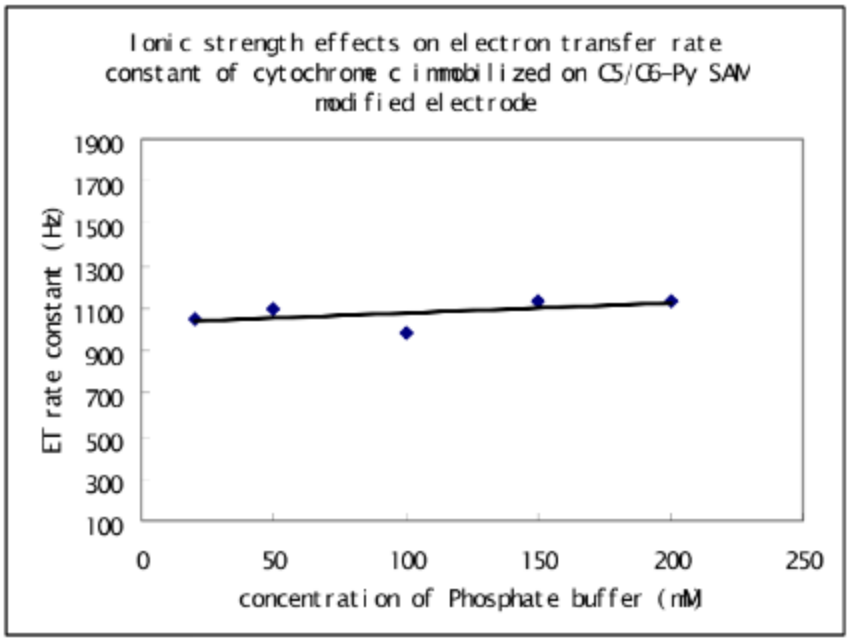

Solutions of different viscosity	k (Hz) 20 mM buffer	k (Hz) 200 mM buffer
0 g/L glucose	1513	1720
200 g/L glucose	1050	1140
400 g/L glucose	672	815

The SAM modified electrodes were incubated in 20 mM buffer solution with 50-100 µM cytochrome c and run cyclic voltammetry in different ionic strength solution by changing the concentration of phosphate buffer at pH 7. The viscosities of the solution were altered by adding 200 g/L or 400 g/L glucose.